Reducing IGBT Losses in ZCS Series Resonant Converters

Gregory Ivensky, Ilya Zeltser, Arkadiy Kats, and Shmuel Ben-Yaakov, *Member, IEEE*

Abstract— **The fundamental operational parameter that controls the losses in series resonant converters was found to be the reflected dc voltage transfer ratio. Losses which are a function of the average current (such as conduction losses of insulated gate bipolar transistors and diodes) are independent of the switching frequency. Losses which are associated with the rms current are a function of both the reflected dc voltage ratio and the switching frequency ratio. Universal and normalized graphs, derived in this paper, can be conveniently used to assess the expected rms and average current conduction losses under any given operational conditions. The residual switching losses in zero-current-switching series resonant converters operating in continuous current mode can be reduced by simple current snubbers placed in the commutation circuits. The experimental results of this paper confirm the theoretical predictions and demonstrate that the turn-on snubbers can reduce switching losses by about 1.5% at a switching frequency of 65 kHz.**

Index Terms— **DC–DC power conversion, insulated gate bipolar transistor, losses, snubber.**

I. Introduction

RESONANT converters have many favorable advantages. They can be designed for zero-voltage switching (ZVS), zero-current switching (ZCS) in either current-fed or voltage-fed topologies. Indeed, they were shown to be useful in a multitude of applications ranging from basic dc–dc converters [1], active power factor correction circuits [2] to capacitor chargers [3], and electronic welders [4]. The main drawback of resonant converter topologies is the higher stresses as compared to pulsewidth modulation (PWM) switchers. This, however, has been ameliorated, to a large extent, since the introduction of economical insulated gate bipolar transistors (IGBT's). Conduction losses of these bipolar devices are mainly a function of the average rather than the rms currents and, hence, high peak currents are not that detrimental. Consequently, resonant topologies still have much to offer.

The main switching limitation of IGBT's stems from the current tail associated with the charge stored in the bipolar junction transistor (BJT) junction of the device [5]. At turn-on, the behavior of the IGBT is similar to that of the MOSFET, i.e., the turn-on transition is mainly dependent on the gate drive and impedance of the control signal path. At turn-off, the IGBT responds slower due to the charge stored in the junction of the IGBT. The complete "off" state is reached only after the charge is completely removed. If the voltage across the IGBT builds up before the charge dissipates, turn-off losses will be high. It is, therefore, advantageous to operate IGBT's in circuits that force the current to zero before the device is turned off. This can be achieved in resonant converters by operating the circuit below the resonance frequency. In these converters, the current through the device reverses before the branch is turned off. This necessitates, in the case of the IGBT, the connection of an antiparallel diode to capture the reverse current. Hence, this mode of operation which is normally referred to as ZCS, appears to be a better strategy for resonant IGBT converters. However, classical resonant converters which operate at frequencies below resonant are still prone to switching losses at turn-on. This is due to the fact that the IGBT's are now hard switched at turn-on. That is, in a typical half-bridge or full-bridge topology, the switch is turned on while the antiparallel diode of the other switch in the same leg is conducting. In this case, turn-on is carried out under hard-switching conditions. Furthermore, high peak current and, hence, high losses are experienced due to the reverse recovery of the diodes. As the switching frequency is increased, these turn-on losses could become significant. Furthermore, the reverse-recovery problem of the antiparallel diodes would be harmful from the EMI point of view. This problem was dealt with in relation to BJT switches [6]–[11] which are slower devices than the IGBT's and, hence, are limited to low switching frequency range. Now that IGBT's are favored, reexamination of this issue with regard to the new switching devices seems to be in order. This was one of the objectives of this paper.

Aside from the question of the residual switching losses, there appears to be a need for a clear delineation of the expected conduction losses in resonant converters. This problem is also not new and has been dealt with in the past. However, we could not find in the literature simple and straightforward answers to the crucial engineering question: what are the expected losses of a resonant converter operating at a given condition? It was, therefore, felt that a fresh look at the problem might contribute to a better understanding of practical limitations of IGBT-based resonant converters.

In this paper, we examine series resonant converters operating below resonance. The objectives were to identify the parameters that affect losses and to examine the possible design tradeoffs. Such information should be useful in the design of this class of converters—considering the fact that every practical design is always a compromise among a multitude of alternatives. To accomplish these objectives, we first

Manuscript received September 29, 1997; revised November 8, 1998. Abstract published on the Internet October 26, 1998.

The authors are with the Power Electronics Laboratory, Department of Electrical and Computer Engineering, Ben-Gurion University of the Negev, Beer-Sheva, 84105 Israel (e-mail: sby@bguee.ee.bgu.ac.il).

Publisher Item Identifier S 0278-0046(99)01080-1.

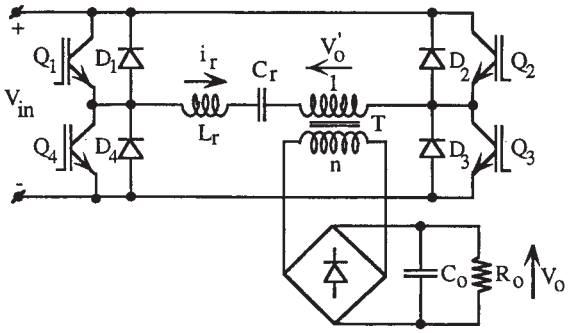

Fig. 1. Basic topology of a voltage-fed series resonant converter.

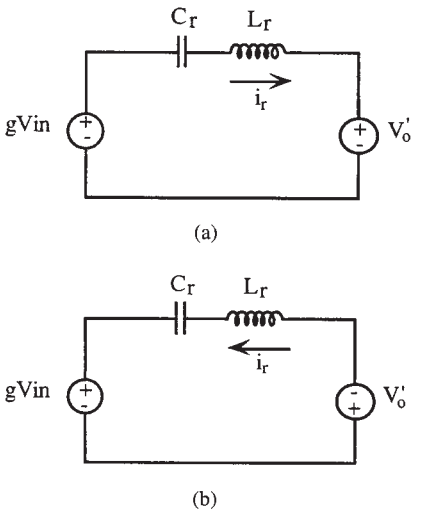

Fig. 2. Equivalent circuits for (a) the transistor conduction interval and (b) for the diode conduction interval.

derive the steady-state relationships, i.e., dc transfer function, peak and average magnitude of the currents, and voltages of power devices, conduction intervals, etc. These are then used to calculate the losses of all power elements, while taking into account that some losses are proportional to the square of the rms currents and others are linear with the average current. The theoretical derivations are then verified against experimental results of a 1-kW converter. Detailed calculations of the expected losses in the experimental converter are given in the Appendix. Finally, general conclusions and design recommendation are given in Section VI.

II. Main Steady-State Equations

Consider a voltage-fed series resonant dc–dc converter (Fig. 1).

Assuming that the switches, diodes, and the transformer are ideal and that the capacitance C_o of the output filter is infinitely high and, therefore, the output voltage V_o is constant, the equivalent circuit for the transistor conduction interval is as given in Fig. 2(a) and for the diode conduction interval as given in Fig. 2(b). Here, V_{in} is the input voltage, g is topology constant ($g = 1$ for full-bridge and $g = 0.5$ for half-bridge), $V_o^{'} = V_o/n$ is the reflected output voltage, and n is the transformer turn ratio (Fig. 1).

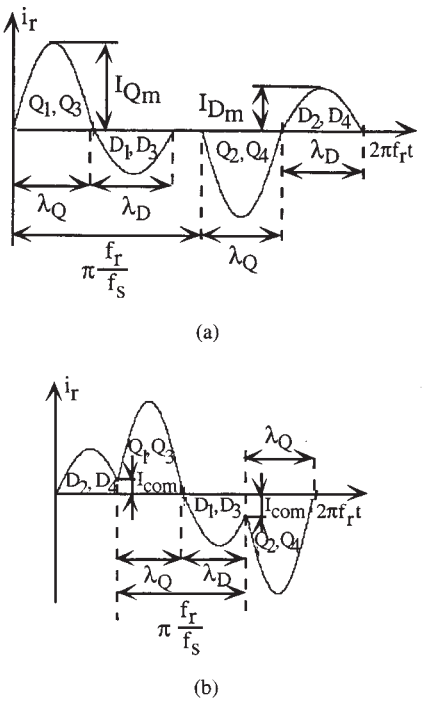

Fig. 3. Resonant current waveform (a) in discontinuous current mode and (b) in continuous current mode.

Both equivalent circuits include the resonant network L_rC_r, but do not include resistors. Therefore, the resonant current i_r consists of ideal sinusoidal segments of the resonant frequency

$$f_r = \frac{1}{2\pi\sqrt{L_rC_r}}. \tag{1}$$

The converter is operating below resonance when the switching frequency f_s is lower than f_r.

We consider the two useful operational modes (Fig. 3): discontinuous current mode (DCM) and continuous current mode (CCM), both under the constraint

$$\frac{2\pi f_r L_r n^2}{R_o} > \frac{4}{\pi}\left(\frac{f_s}{f_r}\right) \tag{2}$$

where R_o is the load resistance. If this inequality is not satisfied, only the transistors are conducting and the reverse diodes do not conduct [8], [11]. In this case, the reflected output voltage is clamped to the input voltage.

DCM [Fig. 3(a)] prevails when

$$f_s < \tfrac{1}{2}f_r. \tag{3}$$

In this mode, the resonant current i_r reaches zero at the end of the resonant period. Consequently, the transistors are turned off and on under ZCS condition. The transistors and diodes conduction angles referred to the resonant frequency (λ_Q and λ_D) are equal to π in DCM.

The converter operates in CCM [Fig. 3(b)] when

$$f_s > \frac{1}{2}f_r. \tag{4}$$

The transistors' and diodes' conduction angles (λ_Q and λ_D) have different values in CCM, but their sum is a function of

the switching frequency ratio

$$\lambda_Q + \lambda_D = \pi \frac{f_r}{f_s}. \tag{5}$$

The transistors' average current $I_{Q\,\mathrm{av}}$ is found to be

$$I_{Q\,\mathrm{av}} = I_{Qm} \frac{(1-\cos\lambda_Q)}{2\pi} \frac{f_s}{f_r} = \frac{I_{\mathrm{com}}}{\pi} \frac{f_s}{2f_r} \tan\left(\frac{\lambda_Q}{2}\right) \tag{6}$$

where I_{Qm} is the peak of the transistors' current and I_{com} is the resonant current at the commutation instant. The diodes' average current $I_{D\,\mathrm{av}}$ is

$$I_{D\,\mathrm{av}} = I_{Dm} \frac{(1-\cos\lambda_D)}{2\pi} \frac{f_s}{f_r} = \frac{I_{\mathrm{com}}}{\pi} \frac{f_s}{2f_r} \tan\left(\frac{\lambda_D}{2}\right) \tag{7}$$

where I_{Dm} is the theoretical peak sinusoidal current of the diodes (real peak when $\lambda_D \geq (\pi/2)$ and asymptotic peak when $\lambda_D < (\pi/2)$). Consequently, the capacitor's peak voltage V_{Cm} is

$$V_{Cm} = \frac{1}{2f_s C_r} (I_{Q\,\mathrm{av}} + I_{D\,\mathrm{av}}). \tag{8}$$

The capacitor's voltage at the commutation instant is

$$V_{C\,\mathrm{com}} = V_{Cm} - \frac{1}{f_s C_r} I_{D\,\mathrm{av}} = \frac{1}{2f_s C_r} (I_{Q\,\mathrm{av}} - I_{D\,\mathrm{av}}). \tag{9}$$

The energy stored in the capacitor C_r during the conduction interval of the transistors and removed during the conduction interval of the reverse diodes

$$\Delta E_C = \frac{C_r}{2} (V_{Cm}^2 - V_{C\,\mathrm{com}}^2) \tag{10}$$

or, applying (8) and (9),

$$\Delta E_C = \frac{1}{2f_s^2 C_r} I_{Q\,\mathrm{av}} I_{D\,\mathrm{av}}. \tag{11}$$

ΔE_C can also be described by two other equations

$$\Delta E_C = (gV_{\mathrm{in}} + V_o') \frac{I_{D\,\mathrm{av}}}{f_s} + \Delta E_L \tag{12}$$

$$\Delta E_C = (gV_{\mathrm{in}} - V_o') \frac{I_{Q\,\mathrm{av}}}{f_s} + \Delta E_L \tag{13}$$

where ΔE_L is the energy stored in the inductor L_r during the conduction interval of the reverse diodes and returned during the conduction interval of the transistors

$$\Delta E_L = \frac{L_r I_{\mathrm{com}}^2}{2} \tag{14}$$

or applying (1), (6), and (7),

$$\Delta E_L = \frac{1}{8\pi^2 f_r^2 C_r} I_{\mathrm{com}}^2 = \frac{1}{2f_s^2 C_r} I_{Q\,\mathrm{av}} I_{D\,\mathrm{av}} N \tag{15}$$

where

$$N = \frac{1}{\tan\left(\frac{\lambda_Q}{2}\right) \tan\left(\frac{\lambda_D}{2}\right)}. \tag{16}$$

Therefore, (12) and (13) can be rewritten as

$$\Delta E_C = (gV_{\mathrm{in}} + V_o') \frac{I_{D\,\mathrm{av}}}{f_s} + \frac{1}{2f_s^2 C_r} I_{Q\,\mathrm{av}} I_{D\,\mathrm{av}} N \tag{17}$$

$$\Delta E_C = (gV_{\mathrm{in}} - V_o') \frac{I_{Q\,\mathrm{av}}}{f_s} + \frac{1}{2f_s^2 C_r} I_{Q\,\mathrm{av}} I_{D\,\mathrm{av}} N. \tag{18}$$

Equating the right sides of (11), (17), (11), and (18), we obtain

$$I_{Q\,\mathrm{av}} = \frac{\omega_s C_r}{\pi} \frac{(gV_{\mathrm{in}} + V_o')}{(1-N)} \tag{19}$$

$$I_{D\,\mathrm{av}} = \frac{\omega_s C_r}{\pi} \frac{(gV_{\mathrm{in}} - V_o')}{(1-N)} \tag{20}$$

where

$$\omega_s = 2\pi f_s.$$

The average input current is

$$I_{\mathrm{in\,av}} = 2g(I_{Q\,\mathrm{av}} - I_{D\,\mathrm{av}}) \tag{21}$$

or applying (19) and (20),

$$I_{\mathrm{in\,av}} = \frac{\omega_s C_r}{\pi} \frac{4gV_o'}{(1-N)}. \tag{22}$$

The normalized average currents of the transistor and diode are, therefore,

$$I_{Q\,\mathrm{av}}^* = \frac{gI_{Q\,\mathrm{av}}}{I_{\mathrm{in\,av}}} = \frac{1}{4}\left(\frac{gV_{\mathrm{in}}}{V_o'} + 1\right) \tag{23}$$

$$I_{D\,\mathrm{av}}^* = \frac{gI_{D\,\mathrm{av}}}{I_{\mathrm{in\,av}}} = \frac{1}{4}\left(\frac{gV_{\mathrm{in}}}{V_o'} - 1\right). \tag{24}$$

The normalized peak of the transistors' current is found from (6) and (23)

$$I_{Qm}^* = \frac{gI_{Qm}}{I_{\mathrm{in\,av}}} = \left(\frac{gV_{\mathrm{in}}}{V_o'} + 1\right) \frac{\pi}{2(1-\cos\lambda_Q)} \frac{f_r}{f_s}. \tag{25}$$

The normalized theoretical peak current of the diode (real when $\lambda_D \geq (\pi/2)$ and asymptotic when $\lambda_D < (\pi/2)$ is found from (7) and (24)

$$I_{Dm}^* = \frac{gI_{Dm}}{I_{\mathrm{in\,av}}} = \left(\frac{gV_{\mathrm{in}}}{V_o'} - 1\right) \frac{\pi}{2(1-\cos\lambda_D)} \frac{f_r}{f_s}. \tag{26}$$

The normalized resonant current at the commutation instant is found from (6) and (25)

$$I_{\mathrm{com}}^* = \frac{gI_{\mathrm{com}}}{I_{\mathrm{in\,av}}} = \frac{\pi}{2} \frac{f_r}{f_s} \left(\frac{gV_{\mathrm{in}}}{V_o'} + 1\right) \frac{1}{\tan\left(\frac{\lambda_Q}{2}\right)}. \tag{27}$$

The reflected output current is related to the transistors' and diodes' currents by

$$I_o' = nI_o = 2(I_{Q\,\mathrm{av}} + I_{D\,\mathrm{av}}) \tag{28}$$

or using (19) and (20)

$$I_o' = \frac{\omega_s C_r}{\pi} \frac{4gV_{\mathrm{in}}}{(1-N)}. \tag{29}$$

The output to input voltage ratio can be found from

$$V_{\mathrm{in}} I_{\mathrm{in\,av}} = V_o' I_o'. \tag{30}$$

Applying (21), (28), and (30), we obtain

$$\frac{V_o'}{gV_{\mathrm{in}}} = \frac{I_{Q\,\mathrm{av}} - I_{D\,\mathrm{av}}}{I_{Q\,\mathrm{av}} + I_{D\,\mathrm{av}}}. \tag{31}$$

We see that $V_o' < gV_{\mathrm{in}}$ as long as $I_{D\,\mathrm{av}} > 0$. For the cases $I_{D\,\mathrm{av}} = 0$, $V_o' = gV_{\mathrm{in}}$.

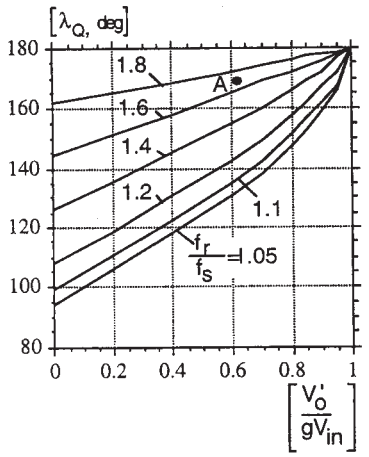

(a)

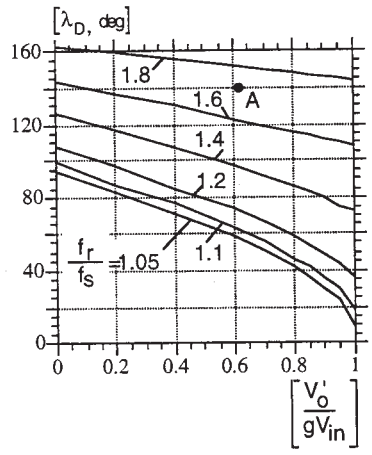

(b)

Fig. 4. (a) Transistors' conduction angle λ_Q and (b) diodes' conduction angle λ_D as functions of dc transfer ratio (V_o'/gV_{in}) for various frequency ratios f_r/f_s (CCM) (*A*: operating point).

Applying (5)–(7) and (31), we find the relationships between the transistors' and diodes' conduction angles (λ_Q and λ_D), the frequency ratio (f_r/f_s), and the output to input voltage ratio (V_o'/gV_{in}) in CCM

$$\begin{aligned}\frac{V_o'}{gV_{\text{in}}} &= \frac{\tan\left(\frac{\lambda_Q}{2}\right)-\tan\left(\frac{\lambda_D}{2}\right)}{\tan\left(\frac{\lambda_Q}{2}\right)+\tan\left(\frac{\lambda_D}{2}\right)} \\ &= \frac{\sin\left(\lambda_Q-\frac{\pi}{2}\frac{f_r}{f_s}\right)}{\sin\left(\frac{\pi}{2}\frac{f_r}{f_s}\right)} \\ &= \frac{\sin\left(\frac{\pi}{2}\frac{f_r}{f_s}-\lambda_D\right)}{\sin\left(\frac{\pi}{2}\frac{f_r}{f_s}\right)}.\end{aligned} \tag{32}$$

The relationships $\lambda_Q = \varphi(V_o'/gV_{\text{in}}, f_r/f_s)$, and $\lambda_D = \varphi(V_o'/gV_{\text{in}}, f_r/f_s)$ of (32) are depicted in Fig. 4.

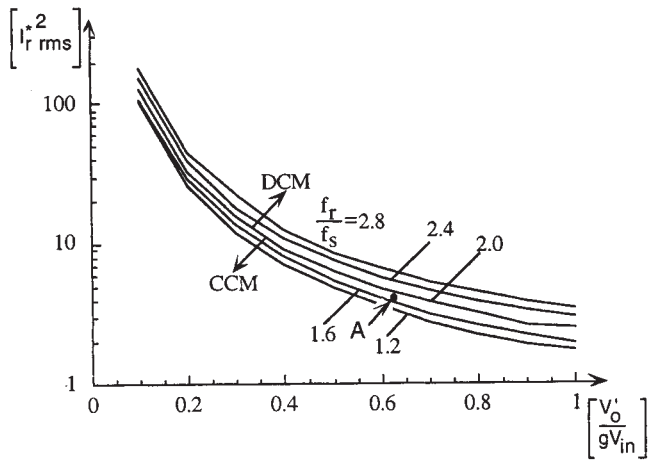

Fig. 5. Effective resonant current (squared) as a function of dc transfer ratio (V_o'/gV_{in}) for various switching frequency ratios f_r/f_s (*A*: operating point).

III. Losses

The losses of the series resonant converter can be grouped as follows:

1) conduction losses of the transformer and resonant inductor;
2) conduction losses of the transistors;
3) conduction losses of the diodes;
4) switching losses of the transistors;
5) switching losses of the diodes.

We first address the issue of conduction losses that are proportional to the rms of the resonant current (type 1 in the above list). To examine this, we derive the rms value of the resonant current $I_{r\,\text{rms}}$ under DCM and CCM using (25) and (26). For DCM,

$$I_{r\,\text{rms}}^* = \frac{gI_{r\,\text{rms}}}{I_{\text{in av}}} = \frac{\pi}{4}\sqrt{\frac{f_r}{f_s}\left[1+\left(\frac{gV_{\text{in}}}{V_o'}\right)^2\right]}. \tag{33}$$

For CCM,

$$I_{r\,\text{rms}}^* = \frac{gI_{r\,\text{rms}}}{I_{\text{in av}}} = \frac{\pi}{2(1-\cos\lambda_Q)}\left(1+\frac{gV_{\text{in}}}{V_o'}\right)\sqrt{\frac{f_r}{2f_s}H} \tag{34}$$

where

$$H = \frac{\lambda_Q}{\pi}-\frac{1}{2\pi}\sin 2\lambda_Q+\left(\frac{\sin\lambda_Q}{\sin\lambda_D}\right)^2\left[\frac{\lambda_D}{\pi}-\frac{1}{2\pi}\sin 2\lambda_D\right]. \tag{35}$$

The above expressions and the relationships shown in Fig. 4 were used to generate curves of the normalized rms resonant current as a function of the dc transfer function with the switching frequency ratio as a parameter (Fig. 5). These curves clearly point to the higher rms-related losses that might be expected when operating in DCM. The rms losses increase when the dc transfer ratio (V_o'/gV_{in}) is reduced (Fig. 5).

An important corollary of the rms loss analysis given above is that MOSFET-based resonant converters will be extremely inefficient due to the very steep increase in rms current. In contrast, conduction losses (P_c) of a diode or IGBT can be

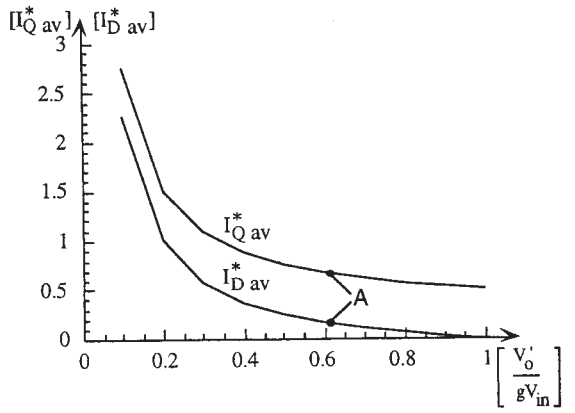

Fig. 6. Average transistors current $I_{Q\,\mathrm{av}}$ and antiparallel diode current $I_{D\,\mathrm{av}}$ as functions of the dc voltage transfer ratio (V_o'/gV_{in}) (*A*: operating point).

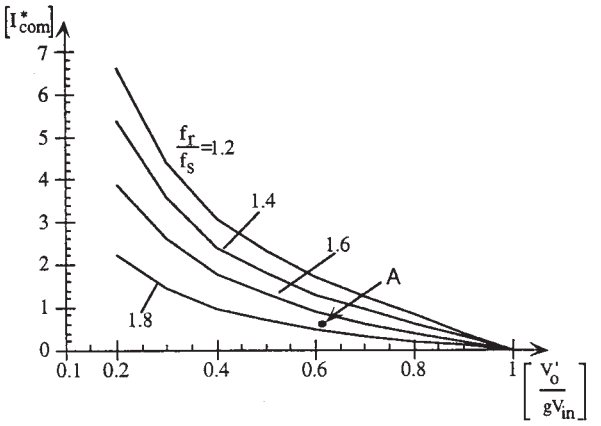

Fig. 7. The commutation current I_{com} as a function of the dc transfer ratio (V_o'/gV_{in}) with the switching frequency ratio f_r/f_s as a parameter (*A*: operating point).

approximately expressed as

$$P_c = I_{\mathrm{av}}\, V_{\mathrm{sat}} \tag{36}$$

where I_{av} is average current through the device and V_{sat} is forward voltage drop. Equations (23) and (24) show that the average currents through the IGBT and through the reverse diode ($I_{Q\,\mathrm{av}}$ and $I_{D\,\mathrm{av}}$) are functions of the dc voltage transfer ratio (V_o'/gV_{in}) and are independent of the frequency ratio f_r/f_s (Fig. 6).

Hence, the rms-related losses of the transformer and the resonant inductor and the losses related to the average current (of transistors and reverse diodes) are strongly dependent on a single fundamental parameter, the voltage transfer ratio (V_o'/gV_{in}). The smaller this ratio, the larger are the losses (Figs. 5 and 6). The rms losses of transformer and resonant inductor are lower in CCM than in DCM. From this aspect, CCM should be preferred. However, in CCM, the hard switching of the IGBT and the reverse diodes pose a severe limitation as the switching frequency is increased. The losses associated with this hard switching will be a function of the magnitude of the resonant current at the commutation instant (I_{com}). The magnitude of this current is related to other variables and parameters of the converter by (27). This equation has been used to evaluate the magnitude of (I_{com}) as a function of the dc transfer ratio with the switching frequency ratio as a parameter (Fig. 7).

IV. Reducing the Turn on Losses

A possible approach to reducing the turn-on losses due to the residual current at the commutation instant is the addition of current snubbers [7]. Some practical implementations are shown in Fig. 8. The addition of the snubbers is chosen to limit the di/dt of the IGBT and diodes.

For the implementation of Fig. 8(a) and (b)

$$\frac{di_Q}{dt} = -\frac{di_D}{dt} = \frac{V_{\mathrm{in}}}{L_\gamma} \tag{37}$$

and for the implementation of Fig. 8(c)

$$\frac{di_Q}{dt} = -\frac{di_D}{dt} = \frac{V_{\mathrm{in}}}{2L_\gamma} \tag{38}$$

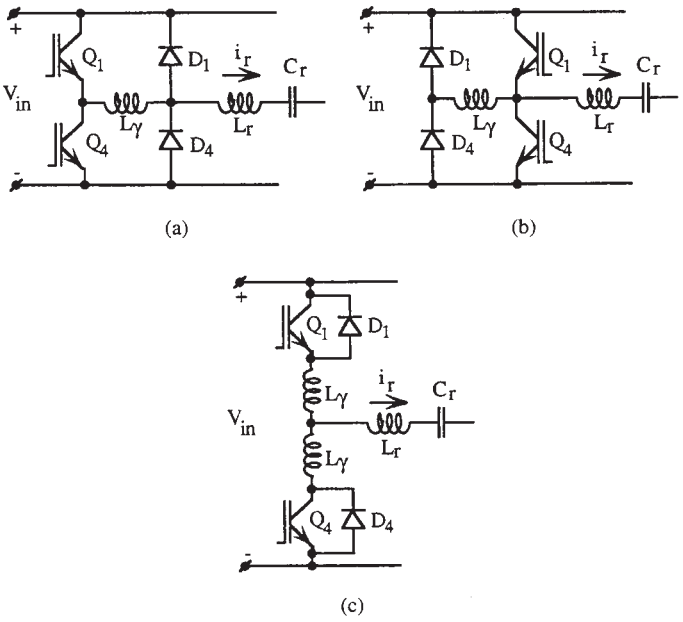

Fig. 8. Possible implementation of turn-on snubbers for ZCS resonant converters.

TABLE I
Maximum IGBT and Diode Voltage in ZCS Converters with Turn-On Snubbers ($\omega_r' = 1/\sqrt{(L_r + 2gL_\gamma)C_r}$)

Topology	$V_{Q\,pk}$	$V_{D\,pk}$
Fig. 8a	V_{in}	$V_{in} + \omega_r' L_\gamma I_{Qm}$
Fig. 8b	$V_{in} + \omega_r' L_\gamma I_{Dm}$	V_{in}
Fig. 8c	$V_{in} + \omega_r' L_\gamma I_{Qm}$	$V_{in} + \omega_r' L_\gamma I_{Qm}$

where L_γ is the inductance of the snubber inductor. The last two equations are obtained under the assumption that the commutation angle is very small compared to the resonant half period. Under this condition, the resonant current i_r stays practically constant during the conduction angle.

The effect of the snubber on the operation of the resonant converter is slight. The snubber inductor will somewhat increase the maximum IGBT voltage $V_{Q\,pk}$ and the maximum diode voltage $V_{D\,pk}$ (Table I).

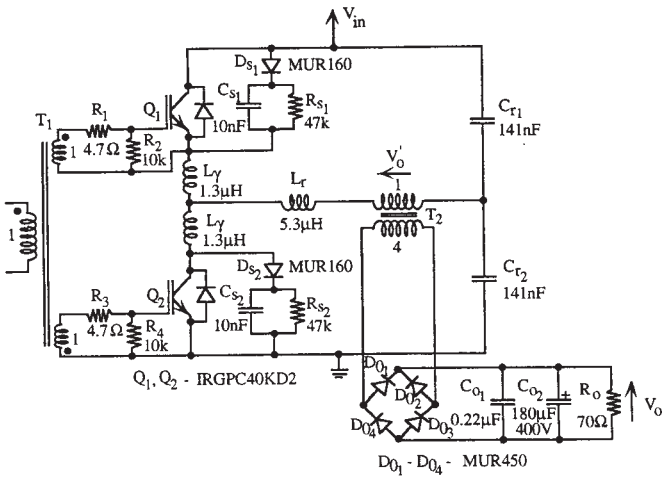

Fig. 9. Schematic diagram of experimental converter.

V. Experimental Results

The results of the theoretical analysis of this paper were verified by testing the performance of an experimental half-bridge resonant converter (Fig. 9). The converter was tested at two frequencies, 65 and 100 kHz. For 65 kHz, $L_r = 5.3$ μH, $C_r = 282$ nF. For 100 kHz, $L_r = 2.3$ μH, $C_r = 282$ nF .

The experimental results confirm the main theoretical conclusion that the IGBT conduction losses are a function of the (reflected) dc voltage ratio and practically independent of frequency. Typical waveforms of the experimental power stage are given in Fig. 10. An efficiency of about 90% was measured under the following experimental conditions: switching frequency 65 kHz, input voltage 198 V, output voltage 243.6 V, and power level 914 W. Losses calculations based on the equations developed in this paper were found to match the measured efficiency to within 0.4 percentage points (see the Appendix). The operating point of experimental converter for which the calculations are given in the Appendix is marked "A" on the plots of Figs. 4–7.

Without the current snubbers, the efficiency dropped from 90% to 88.5%. The efficiency at 100 kHz with the current snubbers for an input voltage of 124 V was about 88%.

VI. Conclusions

The fundamental operational parameter that controls the losses in series resonant converters is the (reflected) dc voltage ratio gV_{in}/V_o'. Losses which are a function of the average current (such as conduction losses of IGBT's and diodes) are independent of the switching frequency. Losses which are associated with the rms current are a function of both the (reflected) dc voltage ratio and the switching frequency ratio. Consequently, when the normalized dc voltage ratio approach unity, the expected efficiency will be the highest.

Universal and normalized graphs derived in this paper can be conveniently used to assess the expected rms and average current conduction losses under any given operating conditions. The switching losses at turn-on of a series resonant converter operating below the resonant frequency in continuous current mode can be reduced by simple current snubbers

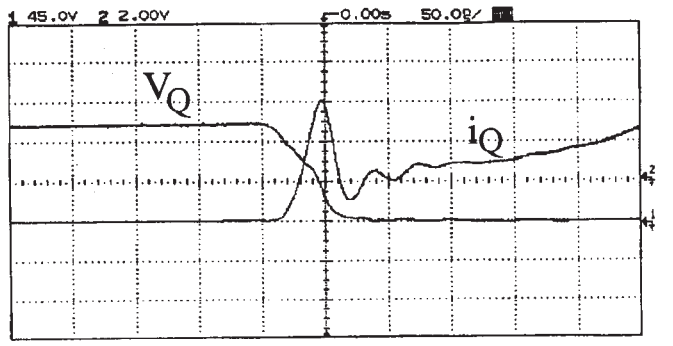

(a)

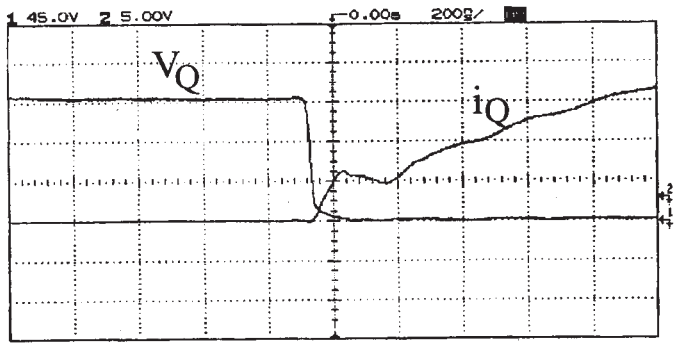

(b)

Fig. 10. Turn-on waveforms of experimental resonant converter when operated at 65 kHz. (a) Hard switching at turn-on, 50 nS/div and (b) with current snubbers [Fig. 8(c)], 200 nS/div.

placed in the commutation circuit. The experimental results of this paper confirm the theoretical predictions and demonstrate that the turn-on snubbers can reduce switching losses by about 1.5% at a switching frequency of 65 kHz.

Appendix
Losses Estimation in the Experimental Converter

Operating Conditions: Switching frequency $f_s = 65$ kHz; input voltage $V_{\text{in}} = 198$ V; and output voltage $V_o = 243.6$ V. The parameters of the converter are marked on Fig. 9.

Measured Data: Leakage inductance of the transformer $L_{lkg} = 0.6$ μH, transformer's resistances: primary $r_{T1} = 0.064$ Ω; secondary $r_{T2} = 0.24$ Ω. Resonant inductor resistance: $r_{Lr} = 0.050$ Ω. Snubber inductor resistance: $r_{L\gamma} = 0.021$ Ω.

Data Taken From a Catalog: Forward voltage drop-transistor IRGPC40KD2 $V_{Q\,\text{sat}} = 2.2$ V, diode MUR450 $V_{D_o\,\text{sat}} = 1.05$ V. We assumed that forward voltage drop of the reverse diodes $V_{D\,\text{sat}}$ is also 1.05 V.

Calculation

Resonant frequency (taken into account L_r, $L\gamma$, L_{lkg})

$$f_r = \frac{10^{-3}}{2\pi\sqrt{(5.3+1.3+0.6)\cdot 10^{-6}\cdot 282\cdot 10^{-9}}} = 111.7 \text{ kHz}$$

$$\frac{f_r}{f_s} = \frac{111.7}{65} = 1.72.$$

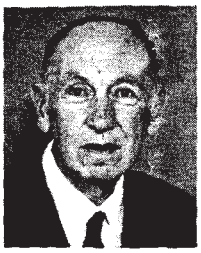

Gregory Ivensky was born in Leningrad, U.S.S.R., in 1927. He received the energy engineer diploma from the Leningrad Railway Transport Institute, Leningrad, U.S.S.R., in 1948 and the Candidate and Doctor of Technical Sciences degrees from the Leningrad Polytechnic Institute, Leningrad, U.S.S.R., in 1958 and 1977, respectively.

During 1951–1962, he was with the Central Design Bureau of Ultrasound and High Frequency Devices, Leningrad, U.S.S.R., and during the period 1962–1989, he was with the Northwestern Polytechnic Institute, Leningrad, where, from 1977, he was a Full Professor in the Department of Electronic Devices. He is presently a Professor in the Department of Electrical and Computer Engineering, Ben-Gurion University of the Negev, Beer-Sheva, Israel. His research interests include power electronic systems such as high-power rectifiers and inverters, induction heating, and dc–dc converters.

Ilya Zeltser was born in Kharkov, Ukraine, in 1971. He received the B.Sc. degree in electrical engineering in 1995 from Ben-Gurion University of the Negev, Beer-Sheva, Israel, where he is currently working towards the M.S. degree in electrical and computer engineering.

He is also carrying out a research program in the Power Electronics Group, Ben-Gurion University of the Negev. His fields of interest include power factor correction methods, snubbers, and dc/dc converter design.

Arkadiy Kats was born in Mariupol, Ukraine, in 1968. He received the B.Sc. degree in electrical engineering in 1995 from Ben-Gurion University of the Negev, Beer-Sheva, Israel, where he is currently working towards the M.S. degree in electrical and computer engineering.

He is currently carrying out a research program in the Power Electronics Group, Ben-Gurion University of the Negev. His fields of interest include dc/dc converter design and integrated magnetics.

Shmuel (Sam) Ben-Yaakov (M'87) was born in Tel Aviv, Israel, in 1939. He received the B.Sc. degree in electrical engineering from the Technion, Haifa, Israel, in 1961 and the M.S. and Ph.D. degrees in engineering from the University of California, Los Angeles, in 1967 and 1970, respectively.

He is presently a Professor in the Department of Electrical and Computer Engineering, Ben-Gurion University of the Negev, Beer-Sheva, Israel, where he is also Head of the Power Electronics Group. He served as the Chairman of the department during the period 1985–1989. His current research interests include power electronics, circuits and systems, electronic instrumentation, and engineering education. He also serves as a consultant to a number of commercial companies on various subjects, including analog circuit design, modeling and simulation, PWM and resonant converters and inverters, soft-switching techniques, and electronic ballasts for discharge lamps.